Astron. Astrophys. 350, 368–378 (1999)

ASTRONOMY AND ASTROPHYSICS

The 408 MHz B3.2 survey

M. Pedani[1,3] **and G. Grueff**[2,3]

[1] Dipartimento di Astronomia, Universitá di Bologna, Via Ranzani 1, 40127 Bologna, Italy
[2] Dipartimento di Fisica, Università di Bologna, Via Ronzani 1, 40127 Bologna, Italy
[3] Istituto di Radioastronomia del CNR, Via Gobetti 101, 40129 Bologna, Italy

Received 25 May 1999 / Accepted 26 July 1999

Abstract. We present a new 408 MHz survey (B3.2) carried out with the "Croce del Nord" radiotelescope in Bologna. The survey coordinates limits are $-2^\circ 00'$ to $+2^\circ 15'$ in Dec. and 21h to 24h, 00h to 17h in R.A., equivalent to 0.388 sr. The B3.2 is complete to 0.15 Jy but many sources down to 0.1 Jy are included. Our aim was to select a new and complete sample of Ultra Steep Spectrum (USS) radio sources, as they proved to be good candidates to find high-z radiogalaxies and their surrounding protoclusters. The observations and the reduction procedure are described and the observational errors are discussed. A cross-identification with the NVSS survey was performed to obtain the spectral index α_{408}^{1400} and radio size of the sources. We found no evidence of a change of the spectral index distribution as radio flux decreases. The B3.2 USS sample contains 185 sources down to 0.1 Jy and it is about one order of magnitude deeper in flux with respect to the 4C USS sample. For 146 B3.2 USS sources no optical counterpart was found on the POSS-I sky survey. A cross-correlation with the FIRST survey gave maps for a subset of 50 USS sources, and their optical ID search was also made on the POSS-II, resulting in 39 empty fields.

Key words: surveys – galaxies: active – radio continuum: galaxies

1. Introduction

The study of powerful high-z radiogalaxies (hereafter $HzRGs$) can yield crucial information on the properties, on the formation epoch and on the evolution of radiosources and their surrounding protoclusters. To this end it is essential to have statistically homogeneous samples. The Ultra Steep Spectrum sources ($S_\nu \propto \nu^\alpha$, somewhat depending on the selection frequency, $\alpha \leq -1$; hereafter USS) of relatively small angular size have been proved over the past years to be good tracers of powerful $HzRGs$. Up to the last year there were about 120 radiogalaxies known with $z > 2$ (de Breuck et al. 1997), but these have been obtained from collection of different datasets, resulting in quite heterogeneous samples, from which it is difficult to derive statistical answers (as stressed by Röttgering et al. 1997). To date, the most distant known AGN is a radiogalaxy with redshift $z = 5.19$ (van Breugel et al. 1999). The radio source was selected from a new sample of ultra-steep spectrum sources and it has an extreme radio spectral index of $\alpha_{365}^{1400} = -1.63$. For a detailed description of the USS properties and of some existing samples see Röttgering et al. (1994). With the "Croce del Nord" radio telescope in Bologna (see Ficarra et al. 1985 for the instrument description) we have performed a new 408 MHz survey, down to 0.1 Jy, tailored to provide an homogeneous and low-frequency selected sample of USS. The survey was made at the lowest declination observable with the "Croce del Nord". The sky area has been chosen so to be easily observed both by northern and southern emisphere optical telescopes. An identical search (Rhee et al. 1996) was carried out over this sky region to select 4C USS but, if we assume a spectral index $\alpha = -1$, the B3.2 USS sample is about one order of magnitude deeper in flux with respect to the 4C USS. Presently it is not known whether this lower flux limit will result in an increased fraction of $HzRGs$ in our survey with respect to the 4C.

The NVSS (Condon et al. 1998) maps have been used to find the 1.4 GHz counterpart of each 408 MHz selected source and to compute the spectral index α_{408}^{1400}.

The present paper provides a description of this Bologna sky survey (to be referred as the B3.2 survey) and of the new USS sample (B3.2 USS). The survey and the data are described in Sect. 2. Sect. 3 deals with the VLA-NVSS maps cross-identification. Consistency and data quality checks are discussed in Sect. 4. In Sect. 5 the B3.2 USS sample radio properties are described, together with preliminary results of the optical identification programme.

2. The B3.2 survey: observations and data

The surveys performed with the "Croce del Nord" radio telescope prior to the B3.2 are summarized in Table 1.

The B3.2 survey has been completed with the same instrumental settings as for the previous B3 survey (Ficarra et al. 1985) but with a different observing and data reduction procedure. In the previous B2 Bologna surveys (Colla et al. 1970) the problems of reduced principal response and of grating response were solved by limiting the beam synthesis to the central part of the primary beam. This procedure however, requires a large num-

Send offprint requests to: M. Pedani (pedani@ira.bo.cnr.it)

Table 1. The radio surveys performed with the "Croce del Nord" radiotelescope at 408 MHz. In the last column, the abbreviations are as follows: Bra65 = Braccesi et al. (1965); GV68 = Grueff & Vigotti (1968); Co70 = Colla et al. (1970); Co72 = Colla et al. (1972); Co73 = Colla et al. (1973); Fa74 = Fanti et al. (1974); Fi85 = Ficarra et al. (1985)

Survey	Lim. Flux (Jy)	# sources	$HPBW$ (arcmin)	Sky coverage	Year	Ref.
B1	1	654	4×108	$3h00m < R.A. < 13h00m(1950)$ $-30^\circ < \delta < -20^\circ(1950)$	1965	Bra65
GV	0.15	328	3×10	$7h40m < R.A. < 18h20m(1950)$ $+34^\circ < \delta < +35^\circ(1950)$	1968	GV68
B2	0.2	3235	3×10	$+29^\circ18' < \delta < +34^\circ02'(1968)$	1970	Co70
B2.2	0.25	3013	3×10	$+24^\circ02' < \delta < +29^\circ30'(1969)$	1972	Co72
B2.3	0.25	3227	3×10	$+34^\circ02' < \delta < +40^\circ18'(1969)$	1973	Co73
B2.4	0.6	448	3×10	$+21^\circ40' < \delta < +24^\circ02'(1969)$	1974	Fa74
B3	0.1	13354	3×5	$+37^\circ15' < \delta < +47^\circ37'(1978)$	1985	Fi85

ber of discrete drift scans to cover a wide declination interval and is more demanding in observing time. In the B3 survey, the problems of reduced principal response and of grating responses were solved by reconstructing the primary beam $BP(\delta)$ for any value of δ, from a discrete sampling of the primary beam itself ($BP(\delta_p)$), obtained by drift scans spaced 30 arcmin. An interpolation with a SINC function made with 8 coefficients revealed to be a good compromise between accuracy and computational effort. As a consequence, the first and the last four drift scans were lost in the interpolation process. In case of the B3.2 survey, it would have been impossible to acquire four scans southward the survey limit $\delta = -2^\circ00'$, as this is the southernmost declination our telescope can observe. Thus, we went back to acquiring more closely spaced scans as in the B2 surveys. At Dec. $\sim 0^\circ$ the 'Croce del Nord' transit radiotelescope has a $3' \times 7'$ HPBW and a sky strip $\sim 45'$ wide in Declination is synthesized in a single scan. Drift scans were obtained spaced by $15'$, allowing a considerable overlap between them. The observations were accomplished between March 1997 and June 1997. Many sky strips have been reobserved because of solar or man-made interference and poor weather conditions. Quality data checks were performed daily at the end of each observation by visual inspection of the calibration source parameters and the overall trend of the total power channels of the sky strip record. If considerable gain fluctuations or interferences were found, the observation was repeated.

The large overlap between contiguous scans yields at least two (or more, if the strip has been reobserved for any reason) independent measurements for any source, taken with different instrumental operating conditions.

This permits a weighted mean of the source parameters (sky coordinates, flux, fit residual) to be calculated. Furthermore, previous observations (Grueff et al. 1980) carried out with the same instrument of 358 sources in the $\pm4^\circ$ strip of the Parkes 2700 MHz survey allow important flux density checks to be done.

As a flux calibrator the source 3C 409 was used, with an adopted $S_{408} = 45$ Jy (see also Sect. 4) and it was observed before the beginning of each strip and after its end. The survey coordinates limits are: $-2^\circ00'$ to $2^\circ15'$ in Dec. and 21h 00m to 24h 00m, 00h 00m to 17h 00m in R.A. (J2000), equivalent to 0.388 sr. However, many sources have been extracted down to Dec. $= -2^\circ15'$ and up to Dec.$= +2^\circ30'$, but in these extended zones the catalogue is incomplete, as discussed later. All the results presented in this paper were obtained considering only the sources within the restricted declination range. The positions and flux densities were measured by a least-squares fitting of the beam function. The synthesis antenna pattern is described as follows:

$$B(\alpha,\delta) = BEW(\alpha,\delta) \cdot BNS(\delta)\, cos(K\alpha + \varphi) \tag{1}$$

where α and δ are the usual astronomical coordinates; BEW and BNS represent the beam function in R.A. and Dec. respectively, and φ represents the phase term between the E-W and the N-S arms due to their structure. The E-W and N-S arms beam functions are thus described:

$$BEW(\alpha,\delta) = \frac{sin(A\,\alpha)}{(A\,\alpha)} \cdot \frac{sin\left(\frac{A}{24}\alpha\right)}{\frac{A}{24\alpha}} \tag{2}$$

$$BNS(\delta) = \frac{sin[A(cos(\delta_0-\gamma))(\delta-\delta_0)]}{8\,sin[\frac{A}{8}(cos(\delta_0-\gamma))(\delta-\delta_0)]} \cdot \frac{sin[\frac{A}{8}((cos(\delta_0-\gamma))(\delta_p-\delta_0)]}{8\,sin[\frac{A}{64}(cos(\delta_0-\gamma))(\delta_p-\delta_0)]} \cdot e^{-\frac{(\delta_p-\delta_0)^2}{\Delta}} \tag{3}$$

In the above formulas, $\gamma = 44^\circ34'21''$ is the Zenith of the North-South arm, δ_0 is the source declination, δ_p is the "primary beam" pointing. Assuming α in units of 4 seconds of time, and $(\delta-\delta_0)$, $(\delta_p-\delta_0)$ in units of 2 arcminutes, the constants A,K,Δ are: $A = 1.5918$, $K = 0.74936$, $\Delta = 1152$. The phase term φ is critical because it varies with the environmental and pointing changes, and it mostly contributes to the source position error in R.A. (an error of 1° in this phase produces a shift of about $1.4''$ in R.A.). We decided to treat it as a free parameter to be fitted together with the source position and flux.

Table 2. The differential B3.2 Log N - Log S, compared to that of the B3 survey. For clarity, the convention adopted for the flux interval boundaries, is shown for the first interval only

Flux Interval Flux Interval	B3.2 counts	B3.2 - av.area	B3 counts	B3 - av.area	B3.2/B3 (-av.area)
[0.1–0.15[	1059	1001	2161	1816	0.55
0.15–0.2	1119	998	1184	995	1.00
0.2–0.3	1141	981	1198	1007	0.97
0.3–0.5	894	788	981	825	0.96
0.5–0.7	325	295	335	282	1.05
0.7–1.0	210	194	236	198	0.98
1.0–1.5	164		166		0.99
1.5–3.0	92		114		0.81
3.0–5.0	35		27		1.30
5.0–10.0	12		13		0.92

The source extraction algorithm worked on each individual map synthetized in a drift scan. A beam function (1) was fitted at each map maximum exceeding a 0.1 Jy value. The fitting algorithm gave position, flux, phase term φ and a fit r.m.s. residual. The fitted source was retained if the ratio flux/residual was larger than 4.6. It is clear that, by accepting sources with inferior ratio, we increase the chance of including spurious sources caused by noise or sidelobe confusion, while requiring a higher ratio could reject real sources. The ratio 4.6 was chosen by comparing the resulting source counts (Log N - Log S) with the accurate determination of the Log N - Log S of the B3 survey (Grueff 1988).

To obtain the Log N - Log S function, an 'avoidance area' has been defined as in Grueff (1988), to eliminate all areas possibly affected by sidelobes of strong sources. The sources with $S_{408} < 1$ Jy which fall inside a flux-dependent cross-shaped area, centered on each source with $S_{408} \geq 1$ Jy, have been flagged and excluded. An additional square area was excluded around those source with $S_{408} \geq 5$ Jy. The total avoided area was 0.062 sr. Table 2 shows a comparison between the B3.2 and B3 differential Log N - Log S. Column 1 contains the flux interval, columns 2 and 4 the sources counts (those of B3 scaled to the lower B3.2 area), columns 3 and 5 the sources counts after the flagged sources in the avoidance areas have been subtracted, and column 6 the ratio of the number counts in columns 3,5 (columns 2,4 for $S_{408} > 1$ Jy). The B3 survey is statistically complete to $S_{408} = 0.1$ Jy and sources down to 70 mJy have been reliably counted outside the avoidance zones. To show the amount of incompleteness in the B3.2 survey, the sources counts ratio in the flux interval $0.1 \leq S_{408} < 0.15$ Jy is reported in Table 2. The B3.2 survey shows an evident and considerable loss of sources at $S_{408} < 0.15$ Jy with respect to the B3 survey. The main cause of this incompleteness is the fact that a threshold of 0.1 Jy for the pixel value was stated for the fitting algorithm. Table 3 shows the mean value of the S/N of the sources (for $S_{408} < 1$ Jy, sources in the avoidance areas have been excluded) calculated for each flux interval. The S/N values in Table 3 are mostly due to confusion, which amounts to about 20 mJy r.m.s. (see Ficarra et al. 1985 for details). The S/N for strong sources

Table 3. The mean value of the S/N for the B3.2 sources

Flux Interval (Jy)	B3.2 - av.area	$\langle S/N \rangle$	$\sigma_{S/N}$
[0.1–0.15[	1001	6.5	< 0.1
0.15–0.2	998	7.7	< 0.1
0.2–0.3	981	10.0	0.1
0.3–0.5	788	13.8	0.2
0.5–0.7	295	20.2	0.5
0.7–1.0	194	25.6	0.9
1.0–1.5	164	34.3	1.2
1.5–3	92	39.2	2.0
3–5	35	47.6	3.4
5–10	12	54.5	8.6

is smaller than implied by this confusion error, because it includes an effect due to sources angular size. For instance, in the 3–5 Jy interval, a 20 mJy confusion error would imply a S/N ratio of 200; the observed lower value of 47.6 is caused by the fact that several sources in this flux interval are sufficiently extended to give comparatively high residuals when fitted with a point-like model. Note that, as shown in Ficarra et al.(1985) (Table 3), confusion errors in the "Croce del Nord" give rise only to random flux errors and no systematic error. As the mean σ for the lowest flux interval is 6.5, we decided not to take into account any correction as in Bennet (1962), and to use the two surveys raw number counts (see also Murdoch et al. 1973). We conclude that the new B3.2 catalogue is statistically complete down to 0.15 Jy with 3999 sources; the number increases up to 5058 at $S_{408} \geq 0.1$ Jy.

If the entire observed declination range is considered ($-2°15' \leq \delta \leq +2°30'$), the number of sources increases to 5578 at $S_{408} = 0.1$ Jy, but the catalogue is no longer complete. In fact, the nominal lowest and highest declination pointings for the center of the strips are $\delta_p = -2°00'$ and $+2°15'$ respectively, and the reduced instrument response, due to the primary beam shape, causes the faintest sources to be lost near the sky strips declination boundaries.

3. The identification with the NVSS sources

To obtain a good measurement of spectral index for the B3.2 sources, we used the NVSS sky survey data (Condon et al. 1998). These data are available both as calibrated sky maps, with pixel size of $15''$ and resolution of $45''$ HPBW, and as a catalogue of sources. We preferred to use the map material, because it allows a better control of the problems arising in the cross-correlation of source catalogues produced at different frequencies and angular resolutions, and differently affected by incompleteness. For instance, if a 0.1 Jy B3.2 source is not found in the NVSS catalogue (which goes down to 2.5 mJy), this implies one of the following: i) a spectral index steeper than about -3; ii) a spurious B3.2 "source", namely a sidelobe or the product of a blend of unrelated sources, due to the relatively poor angular resolution at 408 MHz; iii) incompleteness of the NVSS maps (blanked areas or "holes"). We found that, in the version at our disposal, about 7.3% of map area was missing, i.e. the relative

Table 4. Description of the NVSS cross-ID results

B3.2 sources searched in NVSS	5578 ($S/N \geq 4.6$)
B3.2 sources found	5269
B3.2 sources with bad NVSS fit	83
$\theta \geq 45''$	1380
$\theta < 45''$	3299
BP sources	590
B3.2 sources not found in NVSS	226

pixels were 'blanked'. Of course, this information is missing in the NVSS source catalogue, and to account for it correctly requires to use the map material. We thus developed our own source-measuring algorithm as follows.

A 15×35 pixels matrix is defined around the map pixel corresponding to the B3.2 source position. This rectangular area covers essentially all the B3.2 beam area. A two-component gaussian fit is performed, measuring the stronger source on the map, and approximating the two components with point-like sources. If this fitting gives a source separation less than $15''$, a single point-like component gaussian fit is preferred, and no radio size is given in this case. In each case the total source flux is computed and used to obtain the spectral index. However, if one or more NVSS pixels are 'blanked' (henceforth BP) the whole procedure is skipped, the B3.2 source is marked as BP and it is excluded from further consideration. The statistics of the cross-ID is reported in Table 4.

4. Data quality checks

In the following, checks about the quality of the 408 MHz data will be discussed. It must be noticed however that, though the B3.2 sample has been defined by extracting the sources at the 4.6σ level, we performed the checks using only sources with $S/N \geq 5.2$. This implied excluding 9% of the sources in the lowest complete flux interval considered (0.15–0.3 Jy), but permitted to eliminate most of the spurious 408 MHz sources. In the higher flux intervals, the fraction of the excluded sources is negligible.

4.1. Position uncertainties

The B3.2 radio positions were used to perform the cross-ID with the NVSS maps. Because of the much larger HPBW of our instrument with respect to those of the VLA-NVSS, the 408 MHz positions are certainly affected by much larger errors. The NVSS nominal r.m.s. position error is $\sigma_P \leq 1''$ for strong sources ($S_{1400} \geq 15m$ Jy). As we considered sources with $S_{408} \geq 0.15$ Jy even the sources with the steepest spectra have $S_{1400} \geq 20$ mJy. Thus the B3.2 position errors can be estimated by direct comparison with the NVSS positions. Only the NVSS unresolved sources ($\theta < 45''$) were considered, to avoid possible biases due to the source extension. Figs. 1 and 2 show the histograms of the position differences in the sense B3.2 - NVSS in right ascension and declination.

Table 5. Differences between radio positions (B3.2 - NVSS). Positional errors are in arcsecs

Flux interval (Jy)	# sources	R.A. σ	R.A. offset	Dec. σ	Dec. offset
[0.15–0.3[	1270	17.8	$1.5^{+0.4}_{-0.5}$	19.3	$2.3^{+0.7}_{-0.4}$
0.3–0.5	625	12.7	$0.3^{+0.5}_{-0.6}$	13.4	$3.3^{+0.4}_{-0.5}$
0.5–1.0	411	8.7	$-0.8^{+0.5}_{-0.2}$	9.1	$2.2^{+0.4}_{-0.3}$
1.0–10.0	245	5.9	$-0.6^{+0.3}_{-0.4}$	6.5	$2.6^{+0.6}_{-0.3}$

The distributions are reasonably represented by gaussian functions. Note however that expecially in the lower flux bins ($S_{408} < 0.5$ Jy), the distributions may be considered as the result of two different gaussian components: a relatively narrow gaussian plus a larger gaussian, constituted of those sources with a poor 408 MHz fit and consequent less precise low-frequency positions. For strong sources ($S_{408} > 0.5$ Jy) this effect is smaller as the increasing S/N permits a better position measurement. The dispersion in the position differences is entirely attributable to the B3.2 measurements, and it was estimated as the 68 percentile of the distribution. The systematic offsets contained in our positions were calculated as the median values of the coordinates displacements. Numerical data from Figs. 1 and 2 are listed in Table 5. Columns 3,5 contain the dispersion in R.A. and declination. The R.A. and Dec. offsets are reported in columns 4,6. All the values are in arcsec. The cause of the small but significant declination offset ($\sim 2.6''$) is unknown, but is probably due to the large declination difference between the sky survey region and the calibrator source used. The reason why the R.A. errors are similar to the Dec. errors lies in the fact that, differently to the N-S direction, the interferometer E-W instrumental response contains a term which is subjected to daily phase drifts, as shown in Ficarra et al.(1985). This results in an augmented positional error in the E-W direction, which almost equals that in the N-S direction.

4.2. The B3.2 flux scale

As mentioned in Sect. 2, the B3.2 primary flux calibrator was 3C 409, with an assumed $S_{408} = 45$ Jy. We performed some checks to establish the relationship between our and other flux scales from literature. First, a comparison with fluxes from previous observations (Grueff et al. 1980; hereafter G80) was made. In G80, the 'Croce del Nord' observations of a sample of 358 sources in the $\pm 4^\circ$ declination strip of the Parkes 2700 MHz survey are described. The source 3C 123 was used as flux calibrator with an assumed $S_{408} = 120$ Jy (2% higher than Baars et al. 1977 scale; hereafter Ba77). We considered all the 26 sources with $S_{408} \geq 3$ Jy in G80. The mean ratio B3.2/G80 was 0.98 ± 0.01. The inclusion of sources with $S_{408} \geq 1$ Jy in G80, gave a sample of 78 sources, and a mean ratio B3.2/G80 of 0.99 ± 0.01 (see Fig. 3). Instrumental non-linearity factors (receivers, correlators) were estimated not to exceed 1% at the

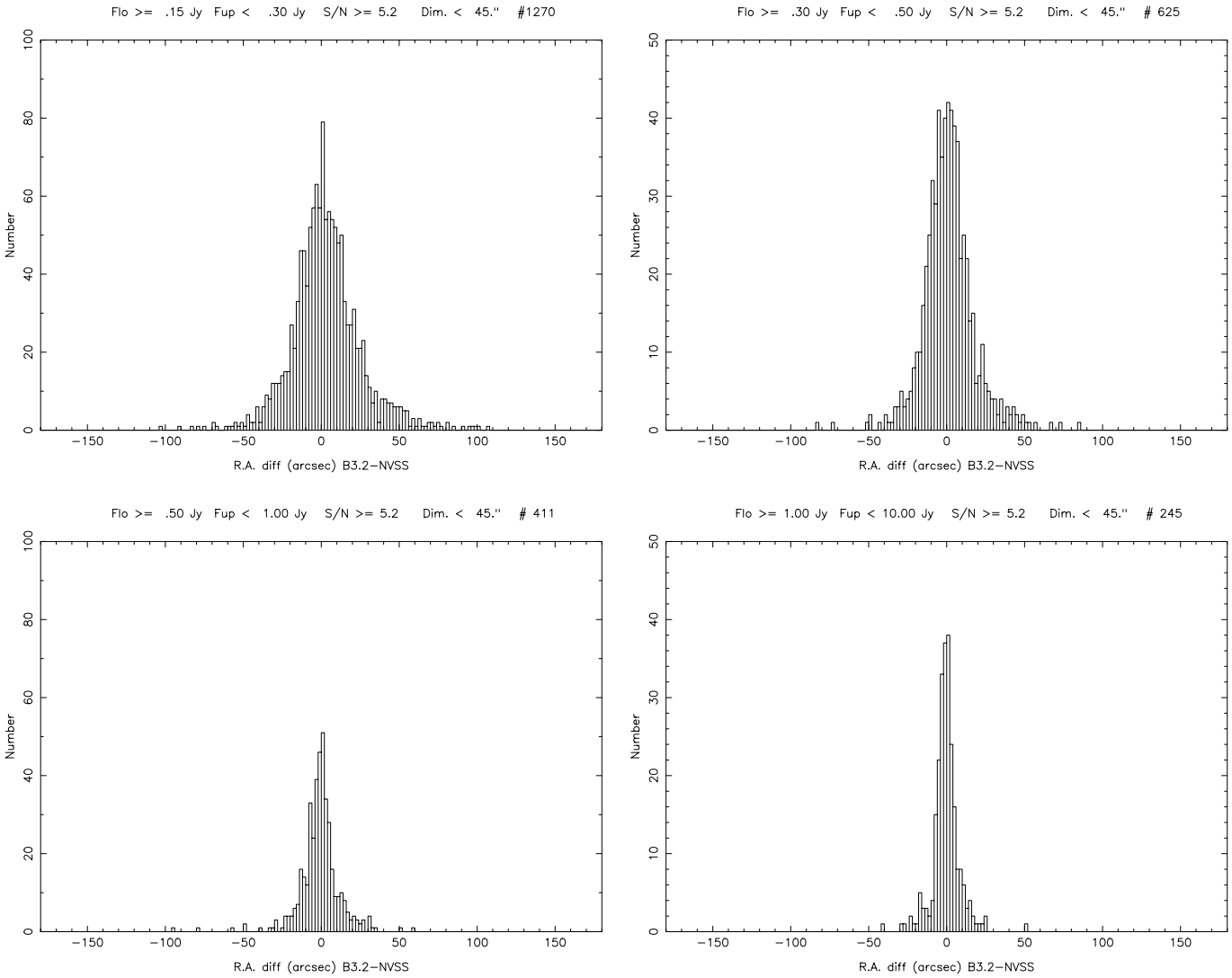

Fig. 1. Differences between right ascensions ($B3.2 - NVSS$) in different intervals of flux (at 408 MHz)

flux level of 3C 123. Thus we can state that the B3.2 flux scale is in accordance with Ba77 to within 1%.

The 408 MHz flux we adopted for 3C 409 flux was derived from past 'Croce del Nord' observations of a set of 3C sources taken from Riley (1988), whose fluxes were scaled to that of 3C 123.

Another flux scale consistency check was made by comparing the B3.2 sources fluxes with those taken from the 408 MHz MRC sample (Large et al. 1981). By positional cross-coincidence, 500 B3.2 sources were found to be common to the MRC sample down to its limiting flux of $S_{408} = 0.7$ Jy. Only the MRC unresolved sources were retained. The mean ratio B3.2/MRC was 0.894 ± 0.005 (see Fig. 4). For the 45 sources with $S_{B3.2} > 3$ Jy, a slightly better accordance was found, with a mean ratio B3.2/MRC $= 0.921 \pm 0.012$. If the sources with $S_{B3.2} \leq 3$ Jy are considered, the mean ratio B3.2/MRC is 0.891 ± 0.005. A nominal difference of 3% is expected to be between the Ba77 flux scale and the Wyllie (1969) flux scale to which the MRC sample refers (Wy69/Ba77 $= 1.03$). Our data show a flux-scale discrepancy of about 11%, the Molonglo fluxes being too high of about 8%. This difference is similar, though less evident, to that found by Fanti et al. (1981) by comparing the B2 flux-scale (2% below Ba77) with that of the MC2 and MC3 (Sutton et al. 1974) catalogues. The mean ratio B2/MC2 found was 0.851 ± 0.006 and was mostly attributed to an error in the Molonglo flux-scale. The same explanation was given by Grueff (1988) to justify why the Log N - Log S counts from MC2 and MC3 were found to be substantially higher than those from the B2 and B3 surveys.

We also considered the possibility of a daily instrumental gain drift to be present in our data, since each observing run lasted 20 hours. For such a test to be performed, literature 408 MHz fluxes of many sources uniformly distributed over the R.A. range covered, would be necessary. As low-frequency data are only available for a limited number of strong sources, we used two alternative methods. The first one consists in subdividing the whole R.A. range into a number of bins to compare the relative sources number counts. We considered sources with

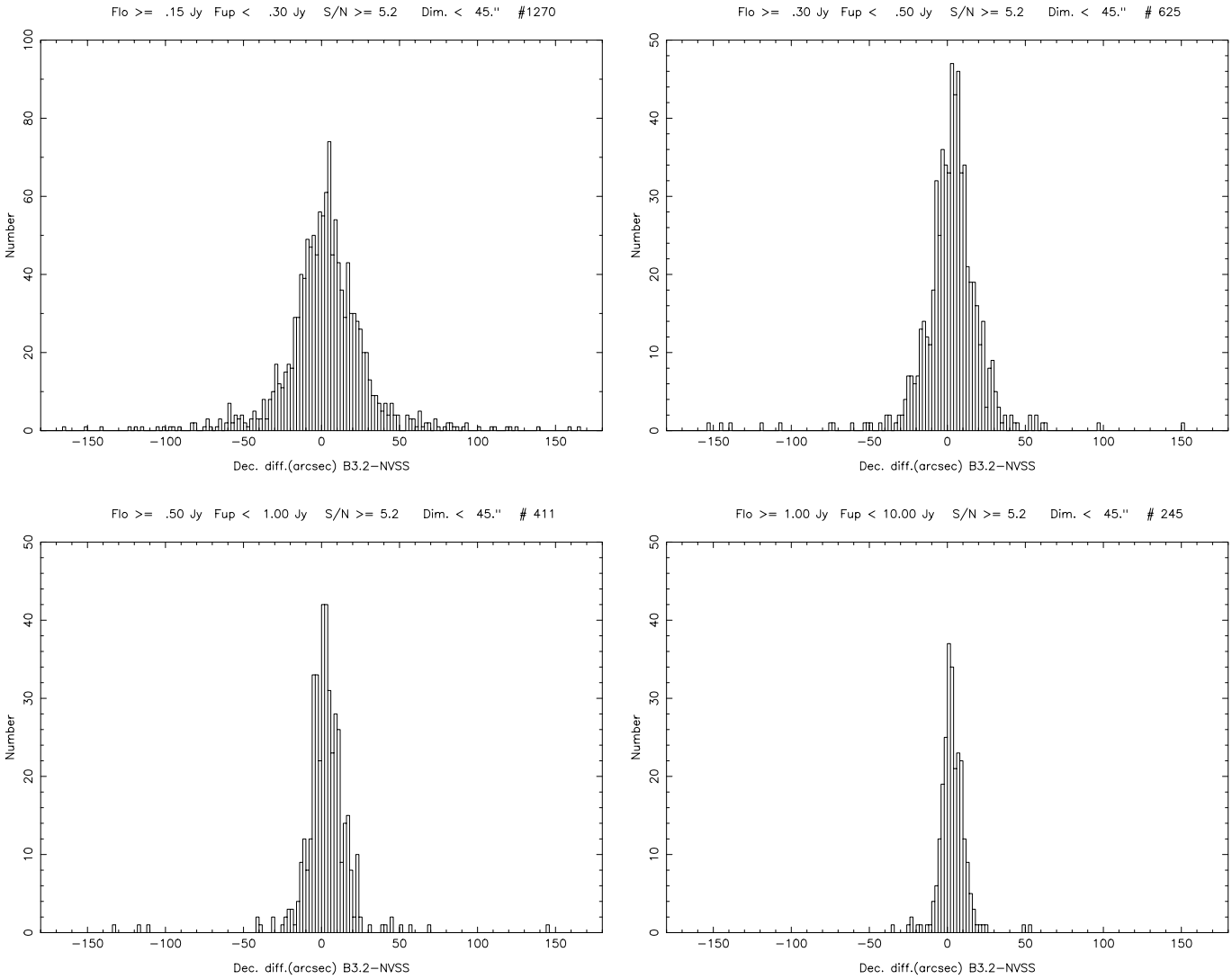

Fig. 2. Differences between declinations (B3.2 - NVSS) in different intervals of flux (at 408 MHz)

Table 6. Median spectral indices for the 4 R.A. intervals

R.A.	# sources	median α_{408}^{1400}
[21h–02h[	928	$-0.80^{+0.015}_{-0.005}$
02h–07h	934	$-0.77^{+0.005}_{-0.010}$
07h–12h	946	$-0.76^{+0.005}_{-0.010}$
12h–17h	956	$-0.81^{+0.010}_{-0.005}$

$S_{408} \geq 0.15$ Jy, $S/N \geq 5.2$ and R.A. boxes 5 hours wide (see Table 6). The obvious assumption of an isotropic sources distribution on the sky is made. We obtained an average of 941 sources per box with a r.m.s. variation of 22 sources, similar to the expected value of 31 ($\sqrt{941}$), indicating a good isotropy and no systematic error affecting flux measurements.

Given a $B3$ integral Log N - Log S slope of 1.06 in the density flux range 0.125–0.4 Jy (the slope for the B3.2 is 1.01 in the 0.175–0.4 Jy flux density interval), a 5% error in flux would imply a variation in the number of sources of about 34 units.

The other method to check for instrumental gain fluctuations is based on the assumption that they give rise to spectral index fluctuations of the sources (see next section).

4.3. Spectral indices

The spectral index distribution of the B3.2 sources is shown in Fig. 5. We can use the spectral index distributions obtained in different R.A. intervals to check for instrumental gain fluctuations. The survey right ascension interval was subdivided into 4 boxes, five hours wide, and the median spectral index was calculated for each box. We considered those sources with $S_{408} \geq 0.15$ Jy, $S/N \geq 5.2$ which have an unresolved counterpart in the NVSS. Spectral data are also reported in Table 6. The median values of α_{408}^{1400} differ up to the 2σ level, indicating a marginal variation with the right ascension. This is substantially in agreement with the result of Sect. 4.2, showing no noticeable

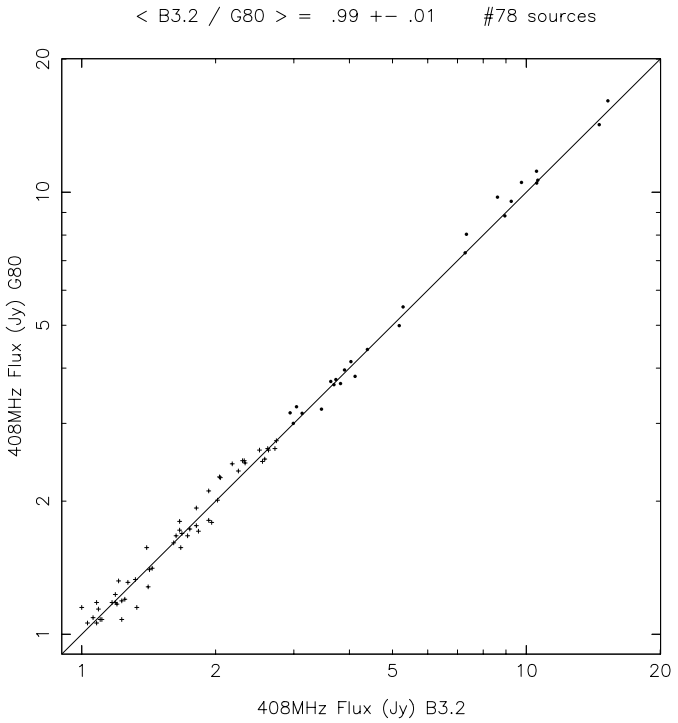

Fig. 3. Flux densities (B3.2 vs G80) for 78 sources; those with $S_{408} < 3$ Jy in G80 are marked with crosses

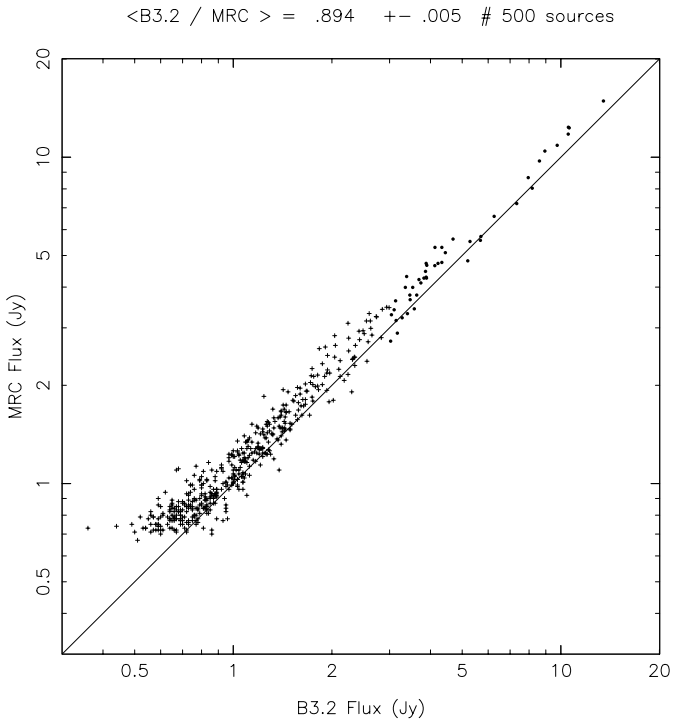

Fig. 4. Flux densities (B3.2 vs MRC) for 500 sources; those with $S_{408} \leq 3$ Jy in B3.2 are marked with crosses

gain change with the right ascension. A change of $\pm 1\%$ in instrumental gain would produce a change of ∓ 0.008 in spectral index.

The existence of a correlation between the flux density and the spectral index could be relevant to the study of the radio sources evolution. Previous works (Grueff et al. 1995 and references therein) did not show any variations of the average spectral index with the flux density in the range $0.03 < S_{408} < 4Jy$. We subdivided the flux range $0.15 < S_{408} < 10\,Jy$ into four bins and we calculated the median spectral index for each flux bin. The straight line (see Fig. 6) is the weighted least-square fit to the data points and the following relation resulted:

$$\alpha_{408}^{1400} = (-0.7697 \pm 0.0060) - (0.0197 \pm 0.0120)\ \log\ S_{408}$$

with a $\chi_\nu = 0.68$. However a fit with an horizontal line gives $\chi^2 \sim 4.5$, corresponding to 20% probability. Thus, we find little evidence of a change in spectral index with the flux.

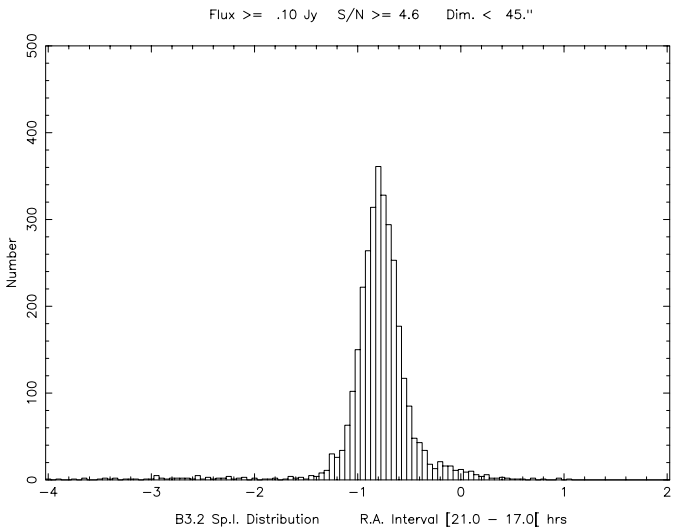

Fig. 5. Spectral indices distribution for the B3.2 sources with $S/N \geq 4.6$ and $\theta < 45''$

5. The B3.2 USS sample

5.1. The sample definition

The selection criteria defining our USS sample are: $S_{408} \geq 0.1$ Jy, $S/N \geq 6.5$, $\theta < 45''$ (as measured on the NVSS maps) and $\alpha_{408}^{1400} < -1$. Furthermore, the zone with R.A 05h 30m to 08h 30m was excluded to avoid low galactic latitude objects (i.e. $|b| < 15°$). Out of a list of 5578 sources, only about 3.3% were retained after applying the selection criteria above, and accurately checking the individual radio data. The B3.2 USS sample thus contains 185 sources. The numerical values adopted for the selection criteria are similar to those used by other groups (Blundell et al. 1998; de Breuck et al. 1997; Rhee et al. 1996). The angular size criterium helps to eliminate relatively nearby objects, objects with 1.4 GHz flux affected by resolution errors, and extended sources dificult to identify optically. There are 2601 B3.2 sources with a NVSS cross-ID, $S/N \geq 6.5$ and $\theta < 45''$ (hereafter B3ID sample) and these provided the 185 USS sample. In the following we try to estimate the number of USS lost because of the various sources of incompleteness.

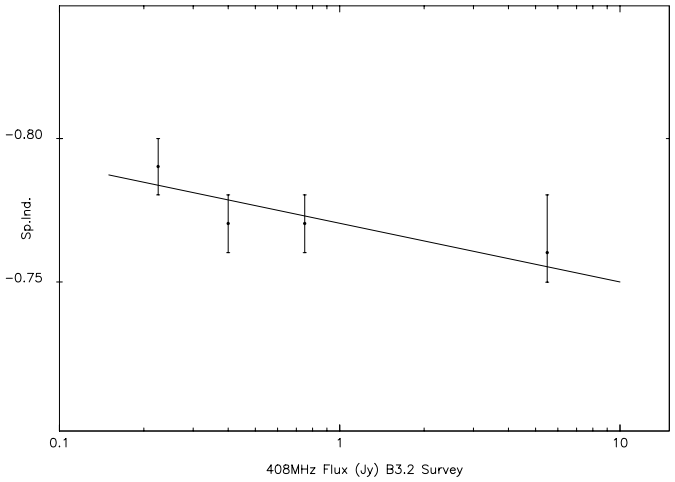

Fig. 6. Median spectral index as a function of flux density

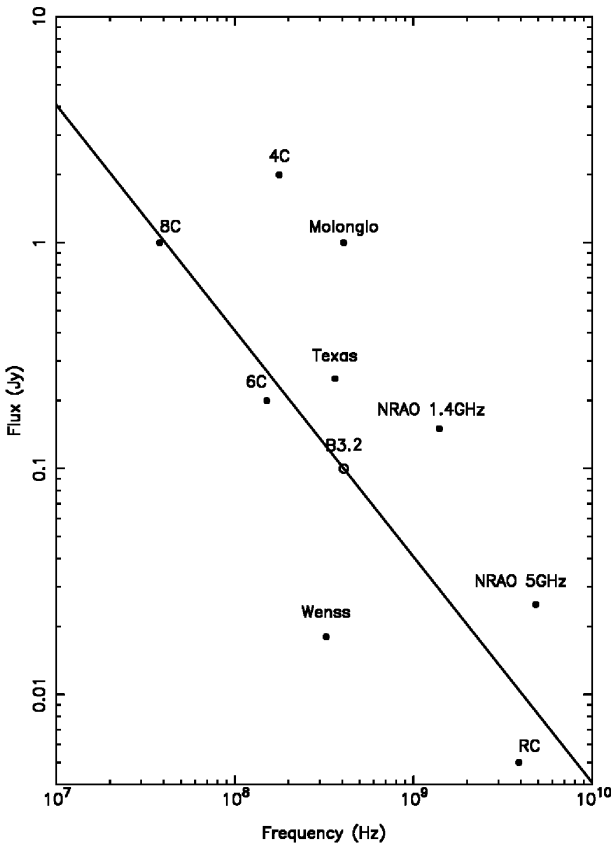

Fig. 7. Low-frequency radio surveys used to derive USS samples. The straight line corresponds to a source with a spectral index $\alpha_{408}^{1400} = -1$, a value adopted in most of cases as a USS selection criterium

There are two important factors which may affect the B3.2 USS sample.

First, the B3.2 survey is statistically complete to $S_{408} = 0.15$ Jy, but the USS have been extracted down to $S_{408} = 0.1$ Jy. From Table 2 (columns 2,4 since for the USS search the avoidance areas have not been considered) and Fig. 7 we calculate that about 13 USS have not been detected in the flux bin 0.1–0.15 Jy because of the B3.2 incompleteness.

Secondly, the presence of BPs on the NVSS maps does not permit the spectral index for a considerable fraction of B3.2 sources to be calculated. Contrarily to the previous one, this factor affects all the USS population, irrespectively of the radio flux. There are 438 BP sources with $S/N \geq 6.5$. As 71% of the sources with a NVSS cross-ID and $S/N \geq 6.5$ have $\theta < 45''$, then out of 438 BP sources, 311 (438×0.71) are expected to have $\theta < 45''$. We expect that out of these 311 BP sources, 25 could be USS lost because of BPs in the NVSS maps.

To conclude, we estimate that about 38 ($13 + 25$) USS have not been detected because of these incompleteness factors.

5.2. The B3.2 USS radio properties

As a first approximation, probing lower fluxes should correspond to sampling more distant objects. Although this zero-order expectation could turn out to be wrong, our survey has been made following this suggestion. To compare the relative sentitivities of the most important low-frequency radio surveys, used to derive USS samples, a plot of the limiting flux versus selection frequency is shown in Fig. 7. With respect to the 4C USS sample (Chambers et al. 1996), the B3.2 USS allows to investigate sources almost one order of magnitude deeper in flux, resulting in a lower intrinsic radio power or possibly a higher redshift for the objects. Moreover, as a radio-optical correlation exists (Tielens et al. 1979, Laing & Peacock 1980), probing low radio powers helps to select those objects with low optical luminosity as well. Their optical emission is thus less contaminated by the AGN nucleus and the surrounding stellar population can be better outlined. Furthermore, a wider coverage of the $P - z$ plane is achieved, with benefits in the statistical study of the radio sources intrinsic properties. Fig. 8 shows the S_{408} distribution for the 4C USS and our sample. For the 4C USS, the S_{408} was obtained by the α_{178}^{1415} or taken from the B3 catalogue when available. The lack of USS with $S_{408} < 1$ Jy is clearly seen in the 4C sample. Note that only 9% of the B3.2 USS have $S_{408} \geq 1$ Jy. The most recent USS sample, selected by a low-frequency survey and also covering the same sky region as our, is the TN sample (de Breuck et al. 1997). It resulted from a cross-correlation of the TEXAS catalogue with the NVSS, adopting a spectral index cut-off $\alpha_{365}^{1400} < -1.3$. As the TEXAS survey (Douglas et al. 1996) is $\sim 80\%$ complete at $S_{365} = 250$ mJy, the B3.2 USS sample contains sources up to two times fainter, and from Fig. 8 we estimate that ~ 50 B3.2 USS have fluxes too faint to have been included in the TN sample.

Fig. 9 shows the spectral index distribution for the 4C USS and B3.2 USS samples. The median α_{408}^{1400} is -1.07 ± 0.01 while the median α_{178}^{1415} is $-1.12^{+0.02}_{-0.03}$. The two distributions are very similar.

Although higher resolution maps are needed to measure precise radio sizes and positions, some statistical considerations may be derived also using the radio sizes given by our fitting algorithm. A comparison between the NVSS catalogue deconvolved sizes and the B3.2 radio sizes for a subset of USS sources,

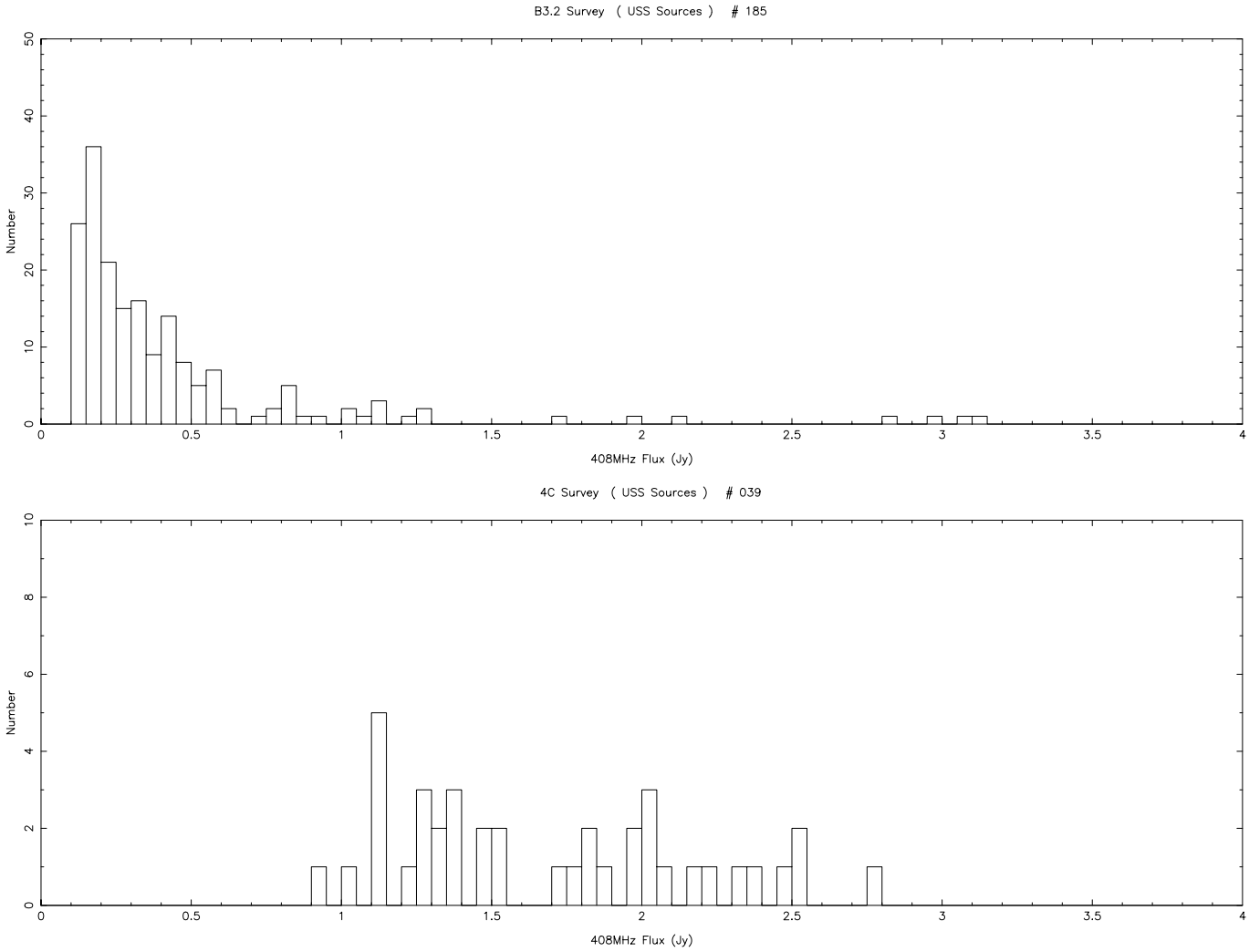

Fig. 8. The S_{408} distribution for the B3.2 sample and 4C USS sources from Tielens et al. (1979) (only sources with $\theta < 45''$ were considered)

showed a substantial agreement within few arcseconds. Out of the 185 USS, 85 were fitted with a double-component model, while the remaining 100 sources (54%) had overall sizes less than $15''$ and were fitted with a single-component model (see Sect. 3). Thus there is indication that about 50% of the B3.2 USS are smaller than 15 arcsec (see Fig. 10). Other authors (Blundell et al. 1998) used much restrictive size selection criteria ($\theta < 15''$) with the aim of retaining the $z > 4$ USS objects in the 6C survey. However, they showed that about 44% of the 3C radiogalaxies, if redshifted to $z = 3$, would be lost because of this size cut. As for the known USS some spread in θ is evident, a too low size cut could make easier the identification process, but it may result in excluding several sources. We compared the size distribution of our USS with that of the existing 365 MHz samples (Röttgering et al. 1994), finding a good agreement.

5.3. The optical ID programme

Because we are interested in selecting only very distant (and thus optically very faint) objects, we firstly examinated the digitized POSS-I red plates to select those USS with no visible optical counterpart. A square box 20 arcsec wide centered at the NVSS position was inspected, resulting in a total of 146 (79%) empty fields (EF) down to $R \sim 20.0$. Any USS with at least one optical object falling inside the box was excluded, irrespectively of it's true optical ID. Consequently, 79% is a lower limit to the fraction of EF in the USS sample. The adopted box size value was derived from very conservative considerations about the NVSS r.m.s. position error, the possible intrinsic radio-optical displacement of a radiosource, and the NVSS maps low resolution.

High resolution (1–2$''$) maps and much deeper optical material are necessary for a secure optical identification. To date, the VLA-FIRST 1.4 GHz (Becker et al. 1995) survey overlaps only in part the B3.2 survey region. We obtained FIRST maps for 50 B3.2 USS, and in most cases, the resolution ($5.4'' \times 6.4''$) is high enough to permit a morphological classification of the sources. For 8 USS, the optical counterpart is visible on the POSS-I plates. For the remaining 42 USS, the optical identification on the deeper POSS-II ($R = 20.8$) was carried out, resulting in one ID, two uncertain cases and 39 are EF. Out of

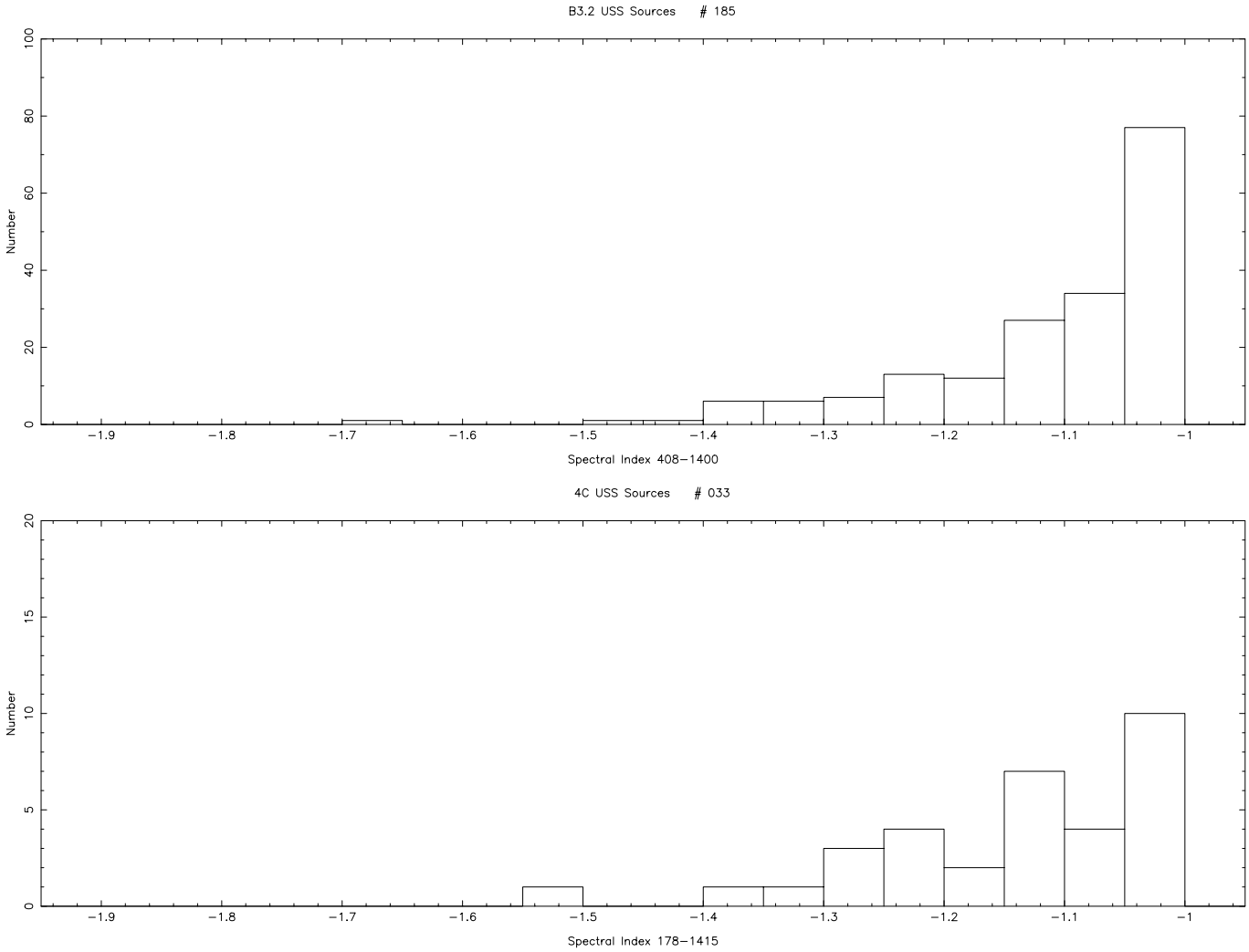

Fig. 9. The spectral index distributions for the B3.2 and 4C USS sample

these 42 USS, 12 are unresolved, 27 are double, 2 are triple and one is a multiple source.

6. Conclusions

This paper describes the first results of an effort to discover high-z radiogalaxies selecting very steep spectrum radiosources.

The technique of the radio spectrum steepness has been exploited by many groups and it revelead to be an effective way to find high redshift radiogalaxies. The present USS sample is about one order of magnitude deeper in flux with respect to the 4C USS sample, and about a factor of two with respect to the recent TN sample (van Breugel et al. 1998) based on the TEXAS 365MHz survey.

In this paper we described the realization of the survey, which was the first step to build-up the B3.2 USS sample, and some details of the observing and reduction procedure. The definition of the B3.2 sources catalogue was obtained by comparison of the Log N - Log S function with that of the previous B3 survey. The B3.2 survey is complete to 0.15 Jy but many sources down to 0.1 Jy are listed giving a total of 5058 sources. A cross-ID with the NVSS 1.4 GHz maps gave us precise radio positions and fluxes to calculate the spectral index α_{408}^{1400}. The radio positions displacement (B3.2 - NVSS) histograms have gaussian shape with a dispersion decreasing from about $15''$ in the flux interval 0.15–0.3 Jy to about $5''$ in the 1–10 Jy interval. Our flux scale is in accordance with that of Baars et al. (1977) to within 1%, while daily instrumental gain drift possibly affecting our data were found to be negligible. We found no evidence of a change of the radio spectrum as flux decreases. As USS selection criteria we used: $\alpha_{408}^{1400} < -1$ and $\theta < 45''$ and these gave a total of 185 sources which constitute the B3.2 USS sample. We started the search of their optical counterparts on the digitized POSS-I plates in order to select only the empty fields to $R = 20.0$. Furthermore, we collected FIRST maps ($5.4'' \times 6.4''$ resolution) for 50 USS sources and we searched for their optical counterparts on the POSS-II prints ($R = 20.8$). For 39 USS no optical ID was found, and out of these, 12 are unresolved in the FIRST maps. The fact that these small sources also have the steepest spectra among the B3.2 USS sources suggests they could reliably be high-z objects.

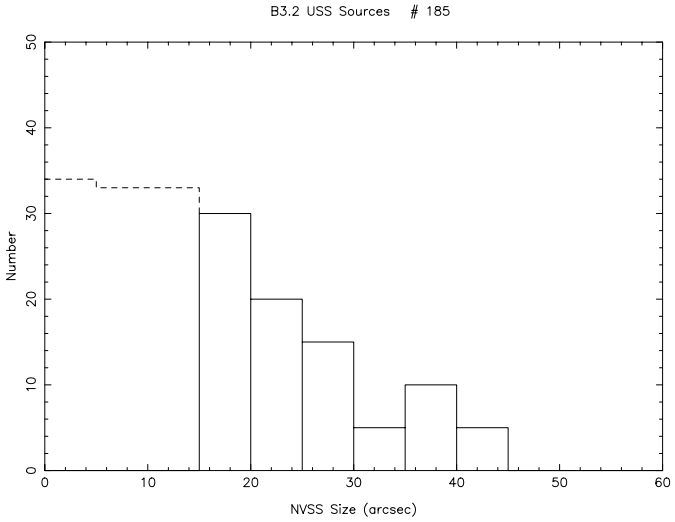

Fig. 10. Distribution of the B3.2 USS sources radio sizes fitted on the NVSS maps. The dashed line encloses the sources with $\theta < 15''$ for which a single component fit was performed

To date, VLA 4.85 GHz observations have been carried out for a subset of 128 B3.2 USS sources, giving $5 \times 4''$ HPBW radio maps and precise flux measurements. For 6 of them, K' band images have been acquired with the new italian telescope TNG during its testing phase. These results will be presented in a future paper. The B3.2 Catalogue is available in digital form via anonymous FTP at the following address: ftp terra.ira.bo.cnr.it; cd /astro/B3.2

Acknowledgements. We want to thank the staff of the Medicina (BO) observing station, particularly Ing. Stelio Montebugnoli, for his help during the observations with the "Croce del Nord" radio telescope. We are also grateful to the referee, Dr. Y. Snellen for helpful comments. This work was partly supported by the Italian Ministry for University and Research (MURST) under grant Cofin98-02-32.

References

Baars J.W.M., Genzel R., Pauliny-Toth I.I.K., Witzel A., 1977, A&A 61, 99
Becker R.H., White R.L., Helfand D.J., 1995, ApJ 450, 559
Bennet A.S., 1962, MNRAS 125, 75
Blundell K.M., Rawlings S., Eales S.A., Taylor G.B., Bradley A.D., 1998, MNRAS 295, 265
Braccesi A., Ceccarelli M., Fanti R., et al., 1965, Il Nuovo Cimento 40, 267
Chambers K.C., Miley G.K., van Breugel W.J.M., Huang J.S., 1996, ApJS 106, 215
Colla G., Fanti C., Fanti R., et al., 1970, A&AS 1, 281
Colla G., Fanti C., Fanti R., et al., 1972, A&AS 7, 1
Colla G., Fanti C., Fanti R., et al., 1973, A&AS 11, 291
Condon J.J., Cotton W.D., Greisen E.W., Yin Q.F., Perley R.A., et al., 1998, AJ 115, 1693
de Breuck C., van Breugel W., Röttgering H., Miley G., 1997, In: Bremer M., et al. (eds.) Searches for High redshift Radio Galaxies: Observational cosmology with the new radio surveys. Conference Tenerife
Douglas J.N., Bash F.N., Bozyan F.A., 1996, AJ 111, 1945
Fanti C., Fanti R., Ficarra A., Padrielli L., 1974, A&AS 18, 147
Fanti C., Ficarra A., Gregorini L., Mantovani F., Olori M.C., 1981, A&A 97, 251
Ficarra A., Grueff G., Tomassetti G., 1985, A&AS 59, 255
Grueff G., 1988, A&A 193, 40
Grueff G., Vigotti M., 1968, Astrophys. Lett. 2, 113
Grueff G., Maccacaro T., Wall J.V., 1980, A&AS 41, 21
Grueff G., Vigotti M., Basso L., 1995, A&A 304, 357
Laing R., Peacock J.A., 1980, MNRAS 190, 903
Large M.I., Mills B.Y., Little A.G., Crawford D.F., Sutton J.M., 1981, MNRAS 194, 693
Murdoch H.S., Crawford D.F., Jauncey D.L., 1973, ApJ 183, 1
Rhee G., Marvel K., Wilson T., et al., 1996, ApJS 107, 175
Riley J.M., 1988, MNRAS 233, 225
Röttgering H., Lacy M., Miley G.K., Chambers K.C., Saunders R., 1994, A&AS 108, 79
Röttgering H., van Ojik R., Miley G.K., et al., 1997, A&A 326, 505
Sutton J.M., Davies I.M., Little A.G., Murdoch H.S., 1974, Aust. J. Phys. Astrophys. Suppl. 33, 1
Tielens A., Miley G.K., Willis A.G., 1979, A&AS 35, 153
van Breugel W., De Breuck C., Röttgering H., Miley G., Stanford A., 1998, In: Morganti R., Couch W.J. (eds.) Looking Deep in the Southern Sky. Proc. of ESO/Australia Workshop, Sydney
van Breugel W., De Breuck C., Stanford A., et al., 1999, ApJ 518, L61
Wyllie D.V., 1969, MNRAS 142, 229